Molecular Properties of Kcv, a Virus Encoded K^+ Channel†

Cinzia Pagliuca,‡,§,|| Tom Alexander Goetze,||,⊥ Richard Wagner,*,⊥ Gerhard Thiel,*,@ Anna Moroni,‡,# and David Parcej§

Dipartimento di Biologia e IBF-CNR, Universitá degli Studi di Milano, Via Celoria 26, 20133 Milano, Italy, Max Planck Institute of Biophysics, Frankfurt, Germany, Institute of Botany, Darmstadt University of Technology, 64287 Darmstadt, Germany, Institute of Biophysics, Department of Biology, University of Osnabrück, Osnabrueck, Germany, and Istituto Nazionale Fisica della Materia, Via Celoria 16, 20133 Milano, Italy

Received July 28, 2006; Revised Manuscript Received November 29, 2006

ABSTRACT: The miniature viral K^+ channel Kcv represents the pore module of all K^+ channels. A synthetic gene of Kcv with an elevated GC content compared to that of the wild-type gene was expressed heterologously in *Pichia pastoris*, and the purified protein was functionally reconstituted into liposomes. Biochemical assays reveal a remarkable cation selctive stability of the channel tetramer via SDS−PAGE. Only cations, which permeate Kcv, were able to protect the oligomer against disassembly into monomers at high temperatures. Electrophysiological characterization of the single Kcv channel reveals a saturating conductance (Λ_{max}) of 360 pS; the single-channel current−voltage relation was strongly rectifying with a negative slope conductance at extreme voltages. The channel was highly selective for K^+ and was blocked by Ba^{2+} and in a side specific manner by Na^+ and Cs^+ also. The channel conducted Rb^+, but as a consequence, the channel was shifted into a hyperactive state. We conclude that specific binding interactions of cations in the conductive pathway are an important determinant of channel stability and function.

Paramecium bursaria Chlorella virus (PBCV-1) (genus *Chlorovirus*, family *Phycodnaviridae*) is a double-stranded DNA virus that infects certain isolates of unicellular eukaryotic *Chlorella*-like alga (*1*). Sequencing the PBCV-1 330 kb genome revealed an ORF (ORF A250R) encoding a small protein of 94 amino acids (Kcv) with similarities to the family of two transmembrane domain potassium (K^+) channel proteins. The predicted transmembrane topology of the protein shows two transmembrane domains (TM1 and TM2) connected by a pore region (P) containing the canonical TXXTXGFG amino acid sequence of the selectivity filter of K^+ channels (*2*). Peculiar to the Kcv protein are a short cytoplasmic N-terminus of 12 amino acids and the absence of a cytoplasmic C-terminus. Thus, Kcv represents essentially only the ''pore module", i.e., a membrane−pore−membrane structure common to all K^+ channels (*3*). Previous studies have established that Kcv forms in spite of its small size a functional K^+ channel in several heterologous systems, including *Xenopus* oocytes (*2*) and mammalian cells (*4*). The selectivity for K^+ and the sensitivity to channel blockers of the Kcv channel in these expression systems resemble those of structurally more complex K^+ channels from eukaryotic organisms, suggesting conserved pore architecture. Kcv even exhibited some voltage dependency, resulting in a moderate inward rectification (*5*). This combination of basic K^+ channel properties with miniature size makes Kcv an ideal model system for examining the minimal molecular architecture and structural requirements for a functional K^+ channel. So far, however, there are no reports about purification of Kcv protein from either natural or overexpressed sources. Although Kcv has been successfully expressed in HEK293 cells and *Xenopus* oocytes, these systems are not suitable for the production of the large amounts of pure protein which are required for structural studies. Furthermore, a steady supply of pure protein is needed to perform functional analysis at a single-channel level. Here we report the successful overexpression of the Kcv gene in the eukaryotic heterologous expression system, *Pichia pastoris*. The channel protein was produced in sufficient quantity for purification to homogeneity, functional reconstitution, and subsequent electrophysiological characterization in an artificial lipid bilayer. Our data show that Kcv protein forms highly stable tetramers. The stability of the functional tetramer is cation specific; K^+ and to some extent also Rb^+ but not Na^+ and Li^+ in the buffer augment the tetramer stability. The purified tetrameric protein could be functionally reconstituted into planar lipid bilayers. The Kcv channel did not exhibit any noticeable anion permeability and displayed a rectifying current voltage relation. The channel was highly selective for potassium ions and was blocked by Na^+, Cs^+, and Ba^{2+} ions. Importantly, the observed single-channel properties of the reconstituted protein allowed us to interpret the macroscopic records obtained after expression in *Xenopus*

† This work was supported in part by the DFG and by Grant RBAU01JT9C from the FIRB Program of the Ministero dell'Istruzione, dell'Università e della Ricerca (A.M.).

* To whom correspondence should be addressed. G.T.: telephone, ++49(0)6151-166050; fax, ++49(0)6151-164630; e-mail, thiel@bio.tu-darmstadt.de. R.W.: telephone, ++49(0)541 969 2398; fax, ++49(0)541 969 2243; e-mail, Wagner@biologie.uni-osnabrueck.de.

‡ Universitá degli Studi di Milano.

§ Max Planck Institute of Biophysics.

|| These authors contributed equally to this work.

⊥ University of Osnabrueck.

@ Darmstadt University of Technology.

Istituto Nazionale Fisica della Materia.

10.1021/bi061530w CCC: $37.00
Published on Web 01/06/2007

oocytes. Finally, the yield of purified protein is such that it opens the possibility for future structural studies.

EXPERIMENTAL PROCEDURES

Escherichia coli strain Topo10F′ (Invitrogen) was used for subcloning and propagation of recombinant plasmids. Protease-deficient *P. pastoris* strain SMD1163 (his4, pep4, prb) (Invitrogen) was used routinely for the expression of the K^+ channel gene. Enzymes for molecular biology were obtained from New England Biolabs or Stratagene. The detergent dodecyl β-D-glucopyranoside (DDM) was from Glycon (Berlin, Germany). DNA sequencing was performed by MWG Biotech. All other reagents were obtained from Sigma Chemical Co. or Merck GmbH, unless otherwise stated.

Manufacture of Expression Constructs and P. pastoris Transformation. Polymerase chain reactions (PCRs) employed either *pfu* I or the Taq Precision Plus System (Stratagene). The sequence of the synthetic gene of Kcv was designed and edited using RESTRI (*6*) and synthesized by Entelchon GmbH (Regensburg, Germany) and inserted into the PCRtopo4 vector. The open reading frame encoding the Kcv synthetic gene was amplified from synthetic Kcv-PCRtopo4 by PCR [forward primer (F1), 5′GACGACGATGACAAGATAATGTTGGTCTTCTCC3′; reverse primer (R1), 5′GGAGAAGACCAACATTATCTTGTCATCGTCGTC3′], introducing a 5′ *Bam*HI restriction site and a 3′ *Not*I restriction site. The PCR fragment was subcloned into *Bam*HI−*Not*I-digested *P. pastoris* expression vector pPIC3.5K (Invitrogen). The construct was confirmed by DNA sequencing.

To aid purification, tag sequences were added to the 5′ end of the synthetic Kcv coding region, to yield the following N-terminus: MAWSHPQFEKTRH(9)D(4)KI, including the Strep II tag, WSHPQFEKTR (*7*), followed by a nonahistidine tag and by the enterokinase cleavage site, DDDDK. *P. pastoris* cells were transformed by electroporation with 15−20 μg of *Pme*I-linearized vectors, using conditions recommended by the manufacturer. After initial selection for His^+ transformants, multicopy integrants were selected by their resistance to increasing concentrations of G418 (Sigma). Clones resistant to 0.2−1.0 mg/mL G418 were selected for further study.

Induction of K^+ Channel Production. Single colonies were grown at 30 °C overnight in MGY medium [0.34% (w/v) yeast nitrogen base, 1% (w/v) ammonium sulfate, 4×10^{-5}% (w/v) biotin, and 1% (w/v) glycerol] to an absorbance at 600 nm (A_{600}) of 2−6. After centrifugation at 1500*g* for 10 min, the pellet was resuspended to an A_{600} of 1.0 in MM medium [0.34% (w/v) yeast nitrogen base, 1% (w/v) ammonium sulfate, 4×10^{-5}% (w/v) biotin, and 0.5% (w/v) methanol] and grown for 48 h. Additional methanol was added after 24 h to a final concentration of 0.5% (v/v), to maintain inducing conditions.

Large-scale cultures were performed in a 5 L fermenter (Labfors III, Infors AG) using a glycerol fed-batch strategy to accumulate biomass prior to induction with methanol (*8*), with sodium hexametaphosphate added as the phosphate source (*9*).

P. pastoris Membrane Preparation. Cells (100 g) were suspended in a final volume of breaking buffer [50 mM sodium phosphate (pH 7.6), 4% glycerol, and 1 mM EDTA] of 100 mL containing 0.1 mg/mL protease inhibitors of soybean trypsin inhibitor, 1 mM benzamidine, and 0.1 mM Pefabloc SC and resuspended using a Poltyron homogenizer (30 s at medium speed). An equal volume of ice-cold, acid-washed glass beads (0.25−0.5 mm diameter) was added, and the mixture was vigorously mixed for 2 min in a Beadbeater (Biospec Instruments). Glass beads, unbroken cells, and other cell debris were removed by centrifugation at 1500*g* for 10 min. The supernatant was removed and centrifuged at 50000*g* for 30 min. The resulting crude membrane pellet was suspended in ice-cold water, and the protein content was determined using the DC protein assay (Bio-Rad). Membranes were diluted with ice-cold water to 20 mg of protein/mL prior to freezing and storage at −80 °C.

Purification of the Kcv K^+ Channel from P. pastoris. Membranes (30 mL) from cells expressing the synthetic Kcv gene construct were detergent-solubilized in buffer containing 50 mM imidazole (pH 7.4), 4% DDM, 600 mM NaCl, and 200 mM KCl for 1 h at 4 °C and cleared by centrifugation (100000*g* for 1 h). The supernatant was loaded (0.5 mL/min) onto 10 mL of Co^{2+}-NTA resin (Qiagen) pre-equilibrated with buffer A. The column was then washed at 1 mL/min twice with 10 mL of buffer containing 50 mM imidazole (pH 7.4), 0.1% DDM, 1 M NaCl, and 200 mM KCl and twice with 10 mL of buffer containing 75 mM imidazole (pH 7.4), 0.1% DDM, and 200 mM KCl. To recover bound protein, the column was eluted at 0.3 mL/min with a buffer containing 300 mM imidazole (pH 7.4), 0.1% DDM, and 200 mM KCl.

Reconstitution of Kcv. The Kcv eluate typically had a protein concentration of ∼20 μg/mL and was reconstituted into liposomes by the addition of 0.09% dodecyl β-D-maltoside (minimum of 99%, Biomol GmbH, Hamburg, Germany) and 10 mg/mL L-α-phosphatidylcholine [from soybean, type IV-S, ≥30% (TLC), Sigma, in 100 mM KCl and 10 mM Mops/Tris (pH 7.0)]. After an incubation time of 30 min, the detergent was removed by the addition of Bio-Beads (SM2 Adsorbent, Bio-Rad). Kcv proteoliposomes were formed overnight at room temperature with three exchanges of Bio-Beads.

Planar Lipid Bilayer. Planar lipid bilayers were produced by the painting technique (*10*). A solution of 80 mg/mL purified azolectin (Sigma, type IV-S) in *n*-decane (Merck, analytical-grade) was applied to a hole (50−100 μm diameter) in a Teflon septum, separating two bath chambers (volume of 3 mL each). The resulting bilayers had a typical capacitance of 0.5 μF/cm^2 and a resistance of >100 GΩ. The noise was 3 pA (rms) at 10 kHz bandwidth. An osmotic gradient of a channel-permeant solute and a channel being in the open state (*11*) are prerequisites for fusion of proteoliposomes with the bilayer. The Ag/AgCl electrodes were connected to the chambers through 2 M KCl−agar bridges. The electrode of the trans compartment was directly connected to the headstage of a current amplifier (Axon Gene Clamp 500B, Axon Instruments, Foster City, CA). Reported membrane potentials are referred to the trans compartment. The amplified currents were digitized at a sampling interval of 0.1 ms and fed into a Digidata1302 A/D converter (Axon Instruments) to store on the hard disk of a personal computer.

Channel transitions between the closed state and full and intermediate conductance states were analyzed with a mean

variance method. The mean current and variance were therefore calculated as an average moving value for a window of 10 data points. Only temporally well resolved gating events describe a full arc with low variance values associated with an open and a closed state. For a positive detection of a gating event, the current level has to be constant for at least 10 data points (i.e., 1 ms at a sampling rate of 10 kHz) before and after the fluctuation. This procedure excludes the possibility that unspecific current spikes due to noise are considered; at the same time, fast and unresolved gating fluctuations are missed.

Remarks on the Terminology "Slow and Fast Block". In general, the reason for K^+ channel block by cations like Na^+, Cs^+, and Ba^{2+} is assumed to be competition for the same binding site rather than an allosteric effect (*12*). In the work presented here, the terms "slow" and "fast" block refer to the definitions described in ref *12*. A fast block is characterized by the apparent reduction of a channel amplitude due to events below the time resolution of data acquisition (10 kHz). A slow block is marked by a shortening of the open channel dwell time or by omission of an open state.

RESULTS

Expression of Kcv Protein in P. pastoris. The wild-type (wt) gene was initially tested for the production of the recombinant protein in *P. pastoris*. Even though several clones were selected, grown, and induced with methanol, production of Kcv recombinant protein was never observed.

It is known that genes with a high A+T content are not efficiently transcribed in *P. pastoris* (*13*, *14*); AT-rich stretches can putatively act as premature transcriptional terminators. Since the AT content of wild-type Kcv is 60% and thus relatively high, we decided to construct a synthetic variant in which the codon usage was optimized for the *P. pastoris* system (*15*). The deduced amino acid sequence of Kcv was reverse translated; codons were replaced with those used in the highly expressed *P. pastoris* alcohol oxidase gene. The resulting nucleotide sequence was then manually edited to increase the GC content to ~50%. In addition, short sequences encoding two tags for purification (StrepII and polyhistidine) and an enterokinase cleavage site were included at the N-terminus. The final construct sequence is shown in Figure 1A. The synthetic gene was transformed into *P. pastoris* cells by electroporation, and the resulting colonies were further selected for multiple genomic insertions (see Experimental Procedures). Western blot analysis using either anti-polyHis or anti-strep antibodies indicated the production of Kcv in the membrane fraction of these cells upon induction with methanol (Figure 1B). Only one band, with an apparent relative molecular mass of 55 kDa, was detected by each antibody. No band was observed in control experiments with cells expressing the empty vector. The value of 55 kDa is considerably higher than the expected value for the Kcv monomer (14 kDa). The observed mass was approximately 4 times that of the monomer, and we speculated that it represented the canonical tetrameric form of K^+ channels (*16*). This hypothesis was confirmed by heating the membranes in the SDS-containing buffer (95 °C for 3 min) prior to electrophoresis. In this case (Figure 1C), a band at 14 kDa, i.e., at the expected molecular mass of the monomer, was observed. For purification, the recombinant Kcv protein was solubilized in DDM. Initial experiments indicated that this detergent was able to maintain Kcv in solution without aggregation. After solubilization with DDM, the recombinant protein was purified on a Co^{2+}-NTA affinity column, because the protein was found to bind the conventional Ni^{2+}-NTA column with only low affinity. A Coomassie-stained gel of a typical purification experiment (Figure 1D, left) shows that most of the contaminant proteins passed through the column, with some extra weakly bound protein removed by the first washing step. The Western blot furthermore shows that only a small fraction of Kcv was found in the flow-through (Figure 1D, right). The Kcv protein could be eluted from the column with a high imidazole concentration (300 mM), resulting in a pure fraction of Kcv protein. Like the membrane-bound Kcv, the pure protein ran at the mass of the putative tetramer (55 kDa) when the sample was not heated. However, unlike in the case of membrane-bound protein, no dissociation into the monomeric 14 kDa fragment was observed upon heating to 95 °C (data not shown), suggesting that the soluble form of Kcv was more stable.

Effect of Monovalent Cations on the Stability of the Kcv Oligomer. To examine the different behavior of membrane-bound and purified Kcv on SDS−PAGE, we investigated the effect of the buffer components on the observed state of oligomerization. Membranes were usually resuspended in pure water, while the purified protein was in a buffer containing 600 mM NaCl and 200 mM KCl. When the membrane preparation was resuspended prior to SDS−PAGE in buffer with the same salt composition that was used for the purified protein (i.e., 600 mM NaCl and 200 mM KCl), the Kcv tetramer appeared to become more stable. Figure 2A shows that the protein ran at an apparent molecular mass of 55 kDa even after heating at 95 °C for 3 min. Further experiments showed that this stability of the tetramer was due to the presence of KCl rather than NaCl in the buffer. When membranes were heated in the presence of only 600 mM NaCl, the channel ran in its monomeric form (14 kDa) (Figure 2A). In contrast, when 200 mM KCl was included in the SDS−PAGE sample buffer, the 55 kDa form was found (Figure 2A). There are at least two possible explanations for the observed effect of KCl on the stability of the Kcv tetramer. First, KCl may act directly on the protein. That is to say, that by binding the channel, K^+ ions strengthen the intersubunit interactions. Second, the effect of KCl could be indirect; it may simply cause depletion of dodecyl sulfate (DS) from the SDS buffer, because the potassium salt of DS is insoluble at room temperature. The latter scenario, however, seems unlikely to account for the observed results since K^+-DS is soluble at 95 °C. Hence, any potential precipitation should be reversed by the heating procedure. Nonetheless, we endeavored to exclude that unspecific effects due to K^+-related precipitation of SDS were responsible for the observed cation specific stability of the oligomer, by performing experiments in which the oligomer stability was tested in nominally identical concentrations of free DS buffers, with and without K^+. To do this, we prepared SDS−PAGE sample buffers containing either 100 or 150 mM SDS. KCl was then added to the two different SDS buffers at concentrations between 0 and 50 mM. If one assumes a 1:1 precipitation ratio of K^+ and DS (*17*), the estimated concentration of free SDS, which is expected to remain after

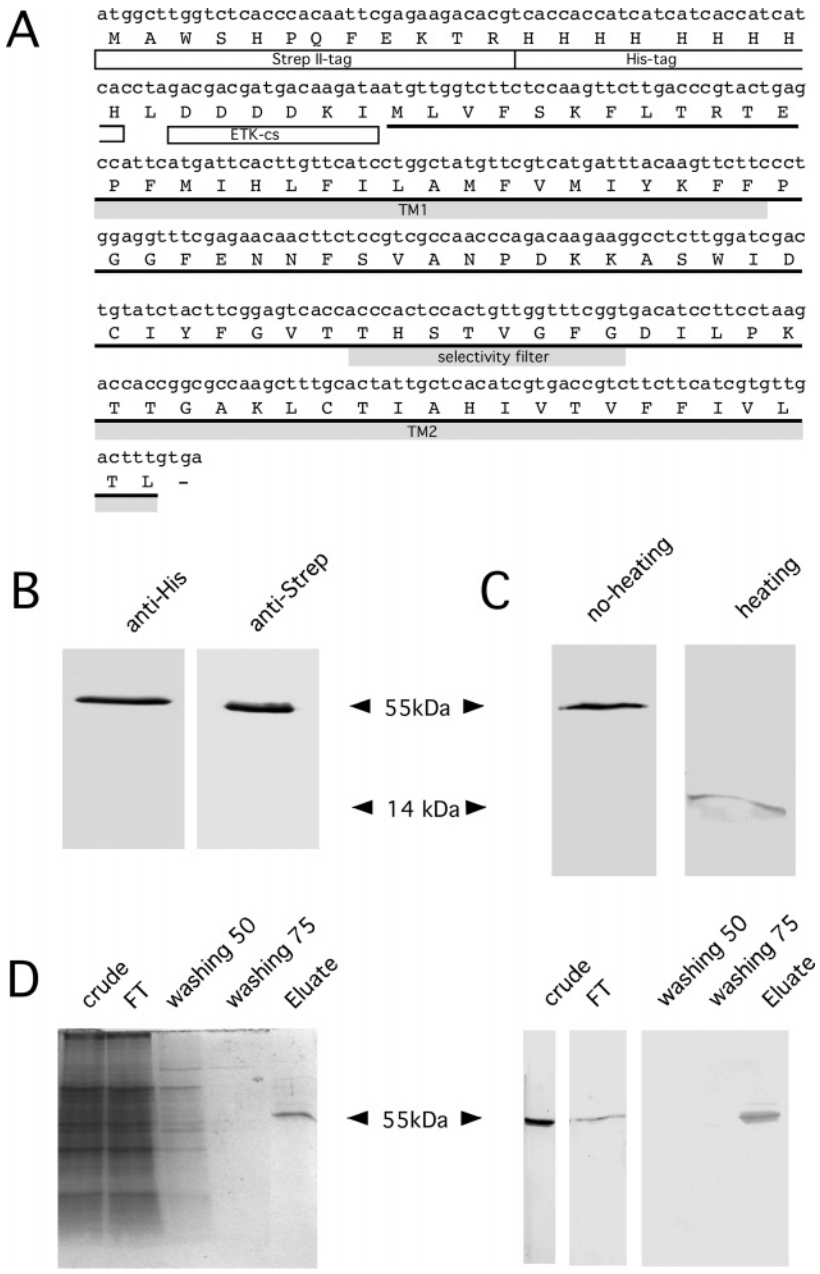

FIGURE 1: Purification of the Kcv protein. (A) Sequence of the synthetic Kcv gene. The sequence carries an N-terminal Strep II tag followed by a nonahistidine tag. The two transmembrane α-helical stretches identified by hydropathy analysis (*2*) are denoted with TM1 and TM2, and the selectivity filter is shaded. In the synthetic Kcv gene, the GC content was increased from an original 40% in the wild type to 49%. (B) Kcv protein production in *P. pastoris* SMD1163 cells. Crude membranes (30 μg of protein) were subjected first to electrophoresis on a 15% SDS gel and then blotted onto a PVDF membrane. Blots were probed with anti-poly-His monoclonal antibody (left) and anti-strepII tag polyclonal antibody (right) and visualized with alkaline phosphatase-coupled secondary antibody. Arrows denote the molecular mass of the tetramer (55 kDa) and the monomer (14 kDa). (C) Effect of heating on the apparent oligomeric state of Kcv on SDS−PAGE gel. Membrane proteins (30 μg) in SDS sample buffer were loaded with (right, heating) or without heating at 95 °C for 3 min (left, no heating). (D) Solubilization and purification of Kcv expressed in *P. pastoris*. Coomassie staining of different purification steps (left) and respective blot of an 8 to 24% acrylamide gradient gel (right). The Western blot was probed with anti-poly-His antibody: lane 1, crude extract (5 μL, 10 mg/mL); lane 2, flow-trough (FT) of the Co^{2+}-NTA column (5 μL, 10 mg/mL); lane 3, washing step with 50 mM imidazole; lane 4, washing step with 75 mM imidazole; and lane 5, one of the eluted fractions.

precipitation with K^+, can be calculated. For example, in Figure 2B, we assumed that when 50 mM K^+ is added to the sample buffer with 150 mM SDS, the free DS concentration drops to a minimum of 100 mM (Figure 2B, outer left lane, bottom panel). With respect to the free SDS concentration, this buffer can therefore be directly compared with the K^+-free 100 mM SDS buffer (Figure 2B, outer right lane, top panel). Comparison of the two experimental conditions shows that the tetrameric form of Kcv (55 kDa band) is found at these nominally identical free DS concentrations only when K^+ is present (Figure 2B). Thus, the different stabilities of the oligomer in the different buffers cannot be explained by a K^+ specific precipitation of SDS. Rather, it is likely to reflect a cation specific effect of K^+ on the channel protein. Previous studies have shown that a cation (e.g., K^+) specific depletion from the solution results in a destabilization and distortion of the selectivity filer in KcsA (*18*). Our observation of a cation specific stabilization of the Kcv oligomer

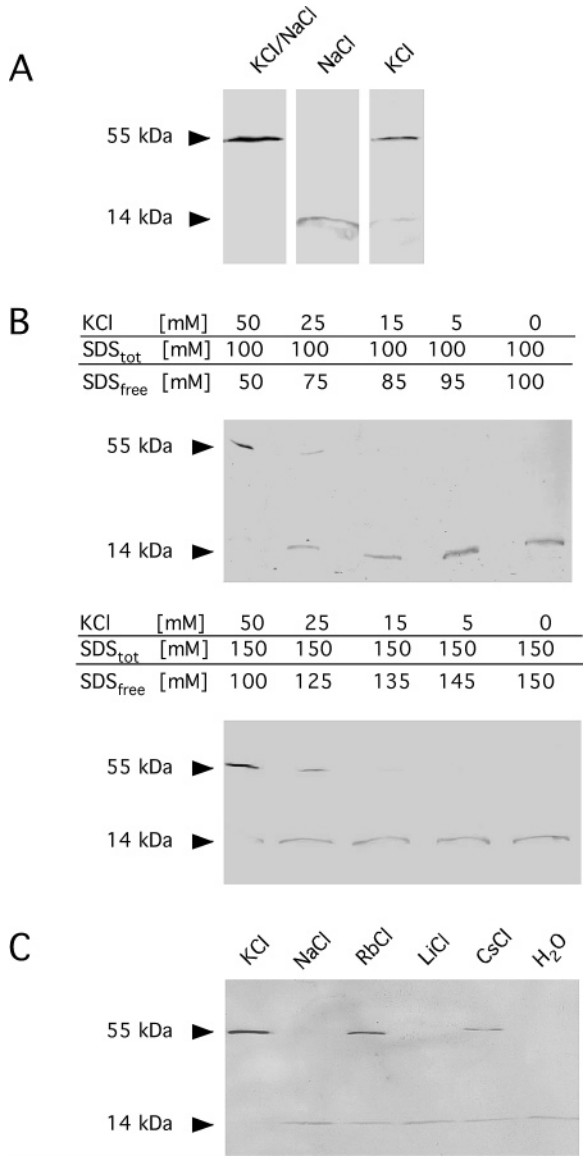

FIGURE 2: Stability of the Kcv tetramer as a function of cations. (A) Cation specific effect on the apparent oligomeric state of Kcv on a SDS−PAGE gel. Membrane proteins (30 μg) were heated for 3 min at 95 °C in a buffer containing 600 NaCl and 200 mM KCl (lane 1), 200 mM KCl (lane 2), or 600 mM NaCl (lane 3). Kcv protein was detected on a Western blot probed with anti-poly-His. (B) Oligomeric state of Kcv in SDS−PAGE as function of free DS. KCl was added at concentrations between 0 and 50 mM to a buffer containing 100 mM SDS (=SDS_{tot}) (top panel) or 150 mM SDS (bottom panel). The resulting free DS concentrations (=SDS_{free}) are shown for each condition and are calculated assuming a 1:1 precipitation ratio of K^+ to DS (*17*). Membrane proteins (30 μg) were heated at 95 °C for 3 min in respective SDS buffer and probed for the oligomeric or monomeric state in a Western blot with anti-poly-His. (C) Like panel A without (H_2O) or with addition of 200 mM monovalent cations.

suggests that the presence of a transportable cation in the filter may enhance oligomer stability. To test this hypothesis, we examined the stabilizing effect of other alkaline cations, which are transported to varying degrees by the Kcv channel (*2*, *3*). Experiments described in Figure 2A were repeated with either Rb^+, Cs^+, or Li^+. The test of oligomer stability shows (Figure 2C) that the permeable cation Rb^+ can largely substitute for K^+. On the other hand, Cs^+, which has a very low channel permeability, exhibits a mixed effect, with the protein distributed roughly equally between monomer and tetramer. The two ions, which are not permeable, Na^+ and Li^+, are unable to protect the oligomer from dissociation upon heating.

Channel Properties of Reconstituted Recombinant Kcv. To examine whether the purified recombinant Kcv protein in its oligomeric state functions as a K^+ channel, we reconstituted the protein into liposomes. These were used for an electrophysiological assay of single-channel activity in planar lipid bilayers. Under symmetrical ionic conditions, fusion of the Kcv liposomes with the bilayer resulted in typical single-channel fluctuations at both positive and negative membrane potentials (Figure 3A). In addition to the main unitary open channel amplitude, the Kcv channel also displayed occasionally diverse sublevel gating (Figure 3D,F). The mean variance plot in Figure 3F illustrates the main transitions between the closed state, two discernible intermediate states, and the full open states. The different states are revealed by data clusters at ~0 pA (closed state), 2 and 5 pA (substates), and 12 pA (fully open state). The transition trajectories between the clusters reveal that channel fluctuations were such that the open state was generally accessed from the closed state. No direct switching between the full and intermediate open levels was detected with a sampling rate of 10 kHz.

The overall open probability of Kcv turned out to be rather low at all voltages (approximately <30%). Even with several channels incorporated into the bilayer, simultaneous opening of two channels was rare.

Figure 3C summarizes the current amplitudes between open and closed forms of the main open state and of the dominant substate as a function of voltage. Provided that only a single active channel had been incorporated into the bilayer membrane, a rectifying single-channel current−voltage relationship was observed (Figure 3C). With multiple incorporated channels, sometimes an additional mirror-inverted curve was observed (data not shown), indicating that the Kcv channels can in principle insert in either direction into the liposome membrane. However, in the majority of the experiments (>80%), the Kcv channels were incorporated with a preferential orientation, yielding the outward rectifying current voltage relation shown in Figure 3C. The rectifying characteristic of the main conductance at negative potentials displays not only saturating behavior but also a negative slope conductance at voltages more negative than approximately −60 mV. This is also observed for the dominant subconductance level at membrane potentials (V_m) of >60 mV (Figure 3C).

In asymmetric buffer with a 10-fold gradient of KCl, the Kcv channel exhibited a zero current potential (V_{rev}) of 50 mV (Figure 3E), indicating an almost perfect cation selectivity of the Kcv channel. The concentration dependence of the linear section of the main conductance state revealed a saturation conductance (Λ_{max}) of 362 pS (Figure 3B).

Channel Block under Bi-Ionic Conditions. Single-channel currents were also measured under bi-ionic conditions. In this case, K^+ was either in the cis or in the trans chamber with another cation (Na^+ or Cs^+) in the opposite chamber. Recordings under a range of bi-ionic conditions (cis/trans, 500 mM each; Na^+/K^+, K^+/Na^+, Cs^+/K^+, and K^+/Cs^+) reveal that the Kcv channel is permeable neither for Na^+ nor for Cs^+ (Figure 4A), with no detectable current for either ion.

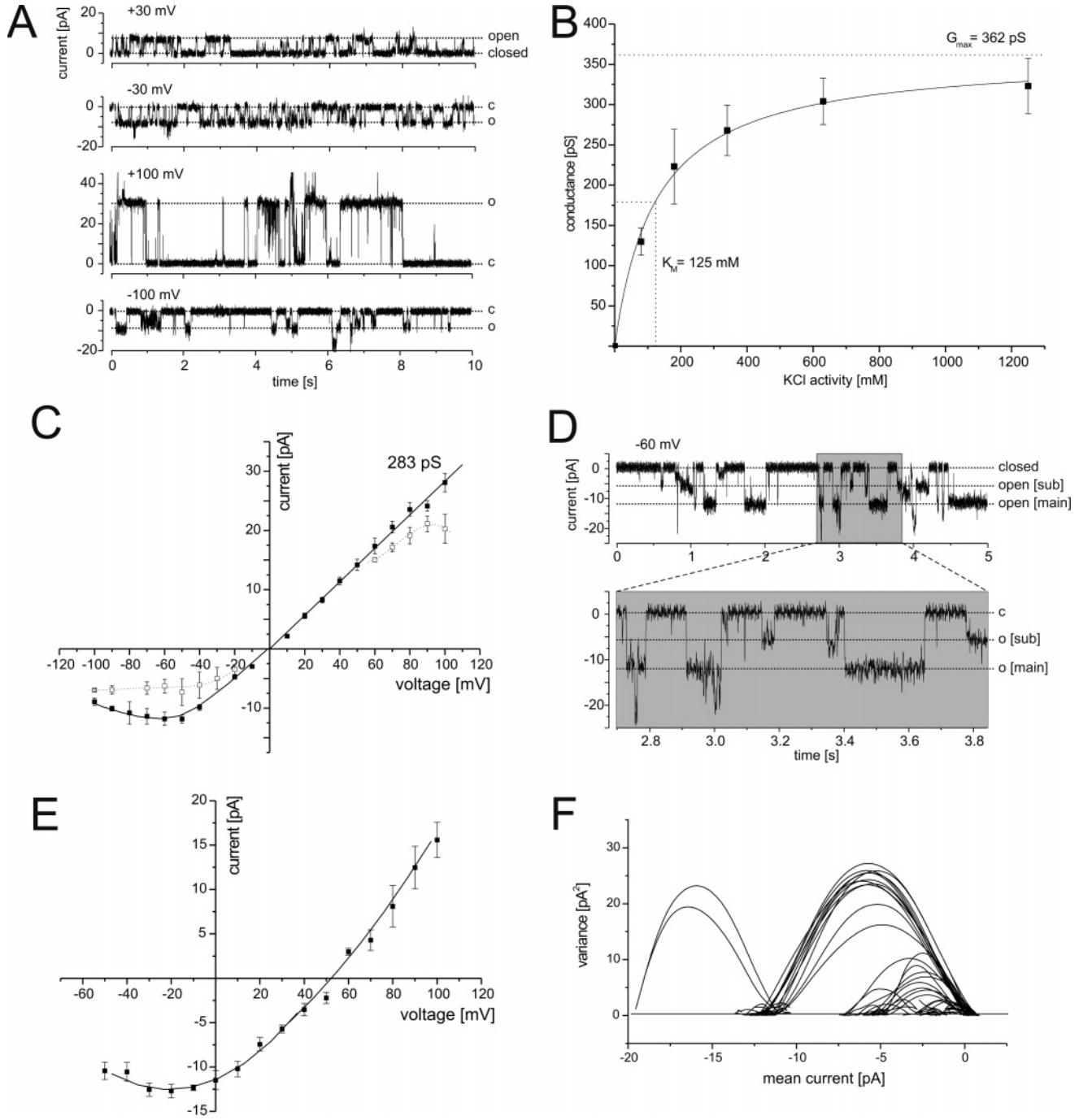

FIGURE 3: Single-channel conductance properties of the reconstituted Kcv protein. (A) Single-channel currents recorded under symmetrical conditions, cis/trans 500 mM KCl with 10 mM Mops/Tris (pH 7.0), at ±30 and ±100 mV. Dotted lines denote corresponding current levels of the closed and fully open conformations of Kcv. A pronounced rectifying behavior becomes obvious when current levels at 100 and −100 mV are compared. (B) Conductance of the Kcv channel at different KCl activities, under symmetrical conditions, cis/trans 10 mM Mops/Tris (pH 7.0) with the indicated KCl activity. Conductance values are based on the slope of the linear section of the *I*−*V* relationship depicted in panel C. Data were fitted with a saturation isotherm, yielding a maximum conductance of ∼360 pS and a half-maximal conductance at 125 mM. (C) Single-channel *I*−*V* relation of the reconstituted Kcv channel in symmetrical cis/trans 500 mM KCl with 10 mM Mops/Tris (pH 7.0) electrolytes. Positive values denote potassium flow from the trans to the cis compartment. Kcv exhibits rectifying behavior with ever-decreasing current amplitudes at very negative potentials. At positive voltages, the *I*−*V* relation is linear. The common main conductance is shown with filled squares, and a subconductance conformation (□) is rarely occupied. In more than 70% of all cases, Kcv was incorporated into the bilayer with the orientation shown. $n \sim 3000$ gating events in 22 independent bilayers. (D) Single-channel currents under the conditions described for panel A with respect of the subconductance state (open [sub]). While the subconductance level is only rarely occupied, the trace shows an unusual frequent occurrence of this state. In nearly all gating events, any open state was accessed from the closed conformation (see also panel F). (E) *I*−*V* relation of Kcv in asymmetrical cis/trans 1 M/100 mM KCl and 10 mM Mops/Tris (pH 7.0) conditions. Kcv exhibits a high selectivity for potassium over chloride with a reversal potential of ∼55 mV. (F) Mean-variance plot of the current trace in panel D. The main conductance state as well as the subconductance state is accessed from the closed state; full and intermediate open states are generally reached directly from the closed state.

Moreover, when only Na^+ was present in the trans compartment, the current carried by K^+ from cis to trans was almost completely blocked [Figure 4A (▼)]. Since K^+ and Na^+ were in opposite chambers, this block cannot be explained by a

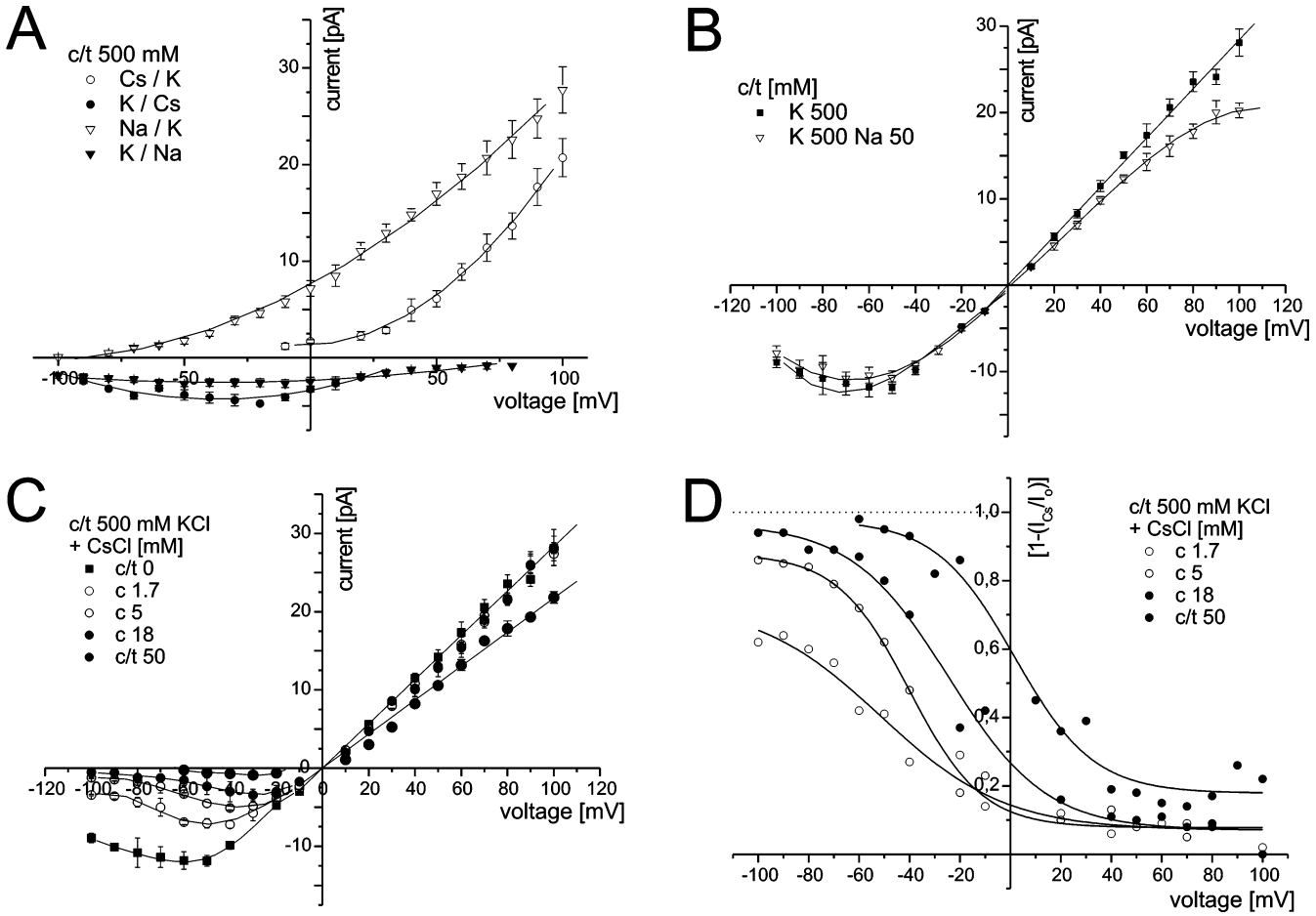

FIGURE 4: Cation selectivity of the reconstituted Kcv channel. (A) Channel activity was recorded under bi-ionic conditions with the cis/trans (c/t) configuration shown in the inset. All $I-V$ characteristics asymptotically approach the voltage axis; this means that Kcv is impermeable for Na^+ and Cs^+ ions. The difference in the $I-V$ relations between the corresponding sodium and cesium experiments can be explained by different abilities for these ions to block Kcv (see panels B−D). (B) Voltage-dependent fast block of Kcv by sodium ions. Channels were assessed in the absence and presence of 50 mM NaCl in a control electrolyte of 500 mM KCl and 10 mM Mops/Tris (pH 7.0). (C) Block of K^+ current by cesium ions. CsCl was successively added to the standard electrolyte [500 mM KCl and 10 mM Mops/Tris (pH 7.0)] in the cis chamber. This revealed a voltage-dependent fast block at negative voltages. The effective inhibitory concentration was below 2 mM CsCl. (D) Relative block of K^+ current by CsCl as a function of voltage. Data from panel C are expressed as the relative block [$=1$ (I_{Cs}/I_0)] and fitted with the Boltzmann equation.

conventional mechanism such as competition of Na^+ and K^+ for the entry or passage of the pore; Na^+ rather blocks the K^+ current at the exit of the channel. We designate this effect as a transmembrane block. Under inverted conditions (cis Na^+/trans K^+), transmembrane block does not occur [Figure 4A (▽)]. For example, the current at 100 mV reaches values comparable to that measured in symmetrical 500 mM K^+ (Figure 3C).

A transmembrane block does also become apparent under bi-ionic conditions with K^+ and Cs^+ in the solution. In this case, however, the effect is apparent for both cis K^+/trans Cs^+ and cis Cs^+/trans K^+ (Figure 4A).

Asymmetry of Cs^+ Block under Symmetrical K^+ Conditions. In further experiments, we examined the effect of Na^+ and Cs^+ when 500 mM K^+ was also included in the buffer. The results of these experiments further illustrate the different effects of Na^+ and Cs^+ on Kcv-mediated K^+ currents. For example, when 50 mM NaCl is added to both chambers in an experiment with symmetric 500 mM KCl, the Na^+ ions cause a voltage-dependent fast block of the current from the trans compartment only (Figure 4B), with the current reduced at positive voltages by up to 20% at 100 mV. Remarkably, Na^+ has under the same conditions no significant impact on the inward current.

Under these conditions, unlike in the bi-ionic setup, Cs^+ blocks the channel currents only from the cis compartment (Figure 4C,D). This fast block occurs in a voltage-dependent manner with a Cs^+ concentration for a half-maximal current reduction [$c(I_{50\%})$] of 2.6 mM (at −50 mV) and 1.2 mM (at −100 mV). This causes the maximal (or peak) current at negative potentials to be shifted from −60 mV when no Cs^+ is added to −30 mV in 18 mM Cs^+.

The asymmetry of the Cs^+ effect [at concentrations up to 50 mM on the trans side, Cs^+ reduces the Kcv current only by roughly 20% (Figure 4C, D)] allows us to assign the orientation of the channel in the membrane of cells which heterologously express Kcv. Previously, it was observed (*2*) that 10 mM Cs^+ ions were unable to block the Kcv channel in *Xenopus* oocyte membranes when it was added from the outside. Thus, it is reasonable to assume that the trans compartment (where no significant Cs^+ block was observed) corresponds to the extracellular side of the membrane. Therefore, we conclude that in the cellular context, Kcv exhibits an inward-rectifying current−voltage relationship.

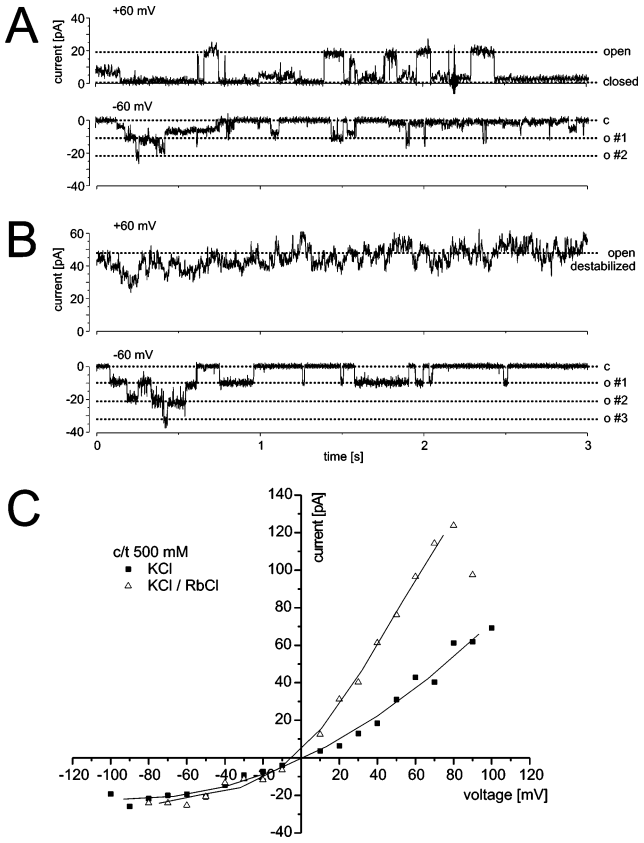

FIGURE 5: Effect of Rb^+ on the conductance properties of the reconstituted Kcv channel. (A) Kcv current trace of a control experiment in the standard electrolyte [500 mM KCl and 10 mM Mops/Tris (pH 7.0)] in cis and trans at ±60 mV. Obvious in panel B is the fact that at least three copies of the channel were incorporated into the bilayer. Dashed lines indicate the closed or fully open state of Kcv. (B) After the standard K^+-containing electrolyte in the trans compartment was replaced with 500 mM RbCl and 10 mM Mops/Tris (pH 7.0), the positive current carried by Rb^+ ions is increased; distinct channel fluctuations are no longer visible. The Kcv channels seem to be destabilized in response to Rb^+ conductance (at a positive voltage) but not K^+ conductance (at a negative voltage). As soon as the current's direction is inversed and carried by potassium ions, the channel regains its "normal" function. (C) $I-V$ relationship of the mean current (1 min) at the respective holding voltages. Data were taken from an equivalent but independent experiment as in panel B. The time-average Rb^+ current is greater than the K^+ current.

Rubidium Currents Carried by Kcv. When under bi-ionic conditions with K^+ and Rb^+ on opposite sides of the membrane, Rb^+ was driven across the Kcv channel by the applied membrane potential, the gating (Figure 5A,B) and open probability of the channel were drastically altered (Figure 5C). Fluctuations to distinct open channel current amplitudes were hardly observed, the channel remaining mainly in the open state. Furthermore, the overall conductance of the open channel increased significantly. This effect was not dependent on the side of the channel to which the Rb^+ was applied. However, although dramatic, the effect of Rb^+ permeation on channel function was readily reversible; when the opposite voltage was applied allowing K^+ to permeate the channel rather than rubidium, the structured gating of the channel reappeared and the open probability returned to control values (Figure 5B, bottom trace). We, therefore, propose that the pronounced effect on the conductance properties of the Kcv channel exerted by permeation of Rb^+ ions is via an effect on the stability of the tetrameric unit as indicated in Figure 2C.

Barium Block of the KCV Channel. To examine the effect of Ba^{2+} on Kcv conductance, the divalent cation was added at different concentrations. Figure 6A illustrates a representative experiment in the absence of Ba^{2+} (top trace) and after addition of Ba^{2+} at 0.66 mM (middle trace) and 4 mM (bottom tace) to the cis chamber. The blocking effect of increasing concentrations of Ba^{2+} on K^+ inward current is summarized in the current−voltage relation in Figure 6C. However, the Ba^{2+} effect was similar if it was added to the trans chamber (not shown). Comparative analysis of the single-channel data in the absence and presence of Ba^{2+} shows that the inhibitory effect of 4 mM Ba^{2+} is due to a slow block of the Kcv channel; the bivalent cation decreases the overall open probability, which in turn can be assigned to a decrease in the open dwell time of the channel (Figure 6B).

Interestingly, in the lower millimolar range an additional voltage-dependent fast block by Ba^{2+} was observed, indicating that at least two different Ba^{2+} binding sites in the Kcv channel are present (Figure 6A, bottom trace). The effects of Ba^{2+} are similar to those recorded with Cs^+ ions but with a slightly lower efficacy. The Ba^{2+} concentration for a half-maximal current reduction [$c(I_{50\%})$] is >4 mM (at −50 mV) and 1.4 mM (at −100 mV).

DISCUSSION

Kcv-mediated currents have already been measured in a variety of heterologous systems by using Kcv cRNA or cDNA (*2*, *4*). In the next step, we sought to measure Kcv activity without any potential impact of modulatory cellular factors. To do this, we needed to produce the channel protein in sufficient amounts to enable reconstitution of the pure channel in well-defined bilayers. Making pure protein also has the attraction of potentially allowing determination of structure−function correlates. Previously, work from one of our labs attempted Kcv gene expression in *E. coli*, but with limited success. *P. pastoris* too initially failed to produce appreciable amounts of protein despite the fact this system has been used for overproduction of the more complex Kv channels (*19*). However, by constructing a synthetic gene chiefly using codons found in the strongly expressed AOX1 gene, we were able to produce significant amounts of Kcv protein, which exhibited channel activity in planar lipid bilayers. This illustrates the importance of the codon usage and AT content of the heterologous gene and may be a useful approach for overcoming poor expression levels for other targets in this system.

Oligomerization and Selectivity Filter. Previous investigations of purified K^+ channel proteins have revealed a high stability and heat tolerance of the channel oligomer (*18*, *20*, *21*). These data show that Kcv shares this remarkable stability with these larger, more complex channel proteins. Interestingly, Kcv lacks significant cytoplasmic domains, which could contribute to oligomer stability (*2*). Hence, the oligomeric association must be based entirely on interactions between the monomers within the membrane bilayer. Even in channels with large extracellular domains, such as Kv proteins, this is also likely to be the case since the removal of cytoplasmic domains does not prevent production of functional tetramers.

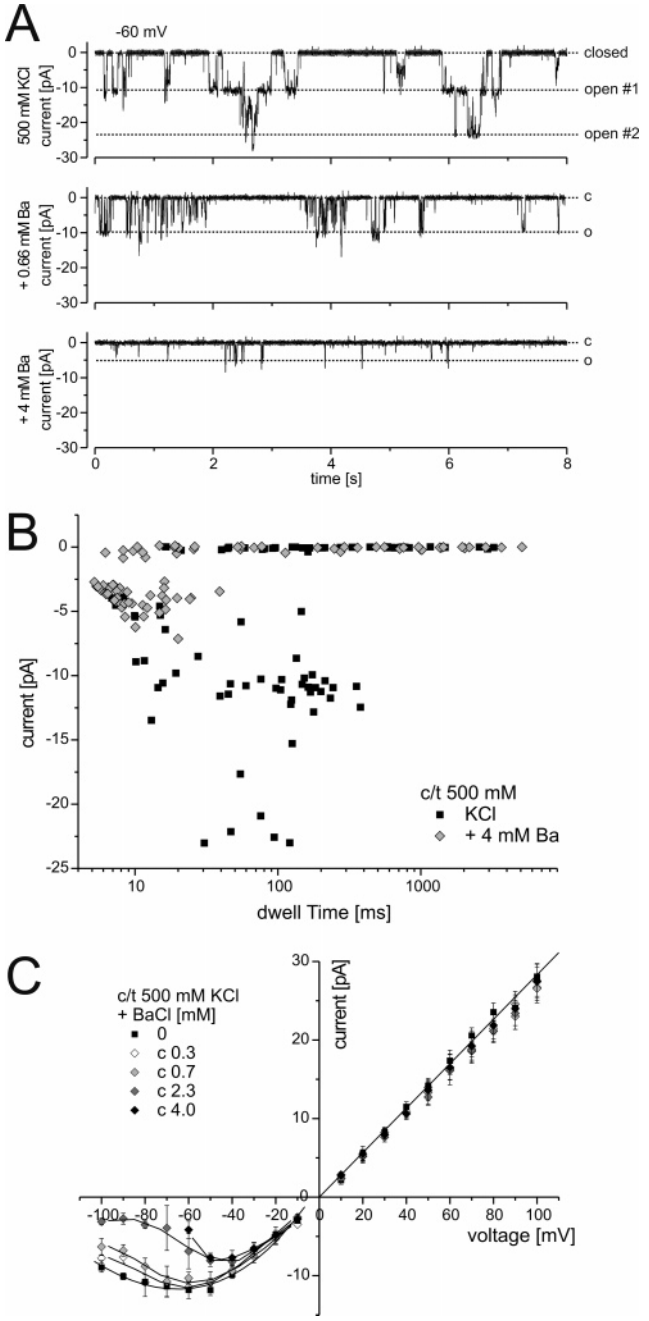

FIGURE 6: Ba^{2+} block of the reconstituted Kcv channel. (A) Current traces of at least two copies of Kcv at −60 mV. Successive addition of BaCl (middle, 0.66 mM; bottom, 4 mM BaCl) to standard electrolyte in cis causes a slow block of Kcv. This is identified by omission of gating events or a reduced dwell time in the open state (see panel B). Barium also induces a fast block of Kcv current at negative voltages (see panel C). (B) Current as a function of dwell time from data in (A, top, no Ba^{2+}; and bottom, 4 mM Ba^{2+}) in a semilogarithmic diagram. In the presence of 4 mM BaCl (gray diamonds), the open channel dwell time does not exceed 40 ms (slow block). Also, the current amplitude does not reach the value recorded in the absence of Ba^{2+} (■); this is evidence for a fast block. (C) *I*−*V* relationship of Kcv currents in the presence of different concentrations of BaCl in cis. Single-channel currents were recorded in the standard electrolyte in the absence and presence of $BaCl_2$ concentrations indicated in the inset. $BaCl_2$ leads to a concentration- and voltage-dependent fast block. The blocking effect is much smaller when BaCl is added to the trans chamber (<20% relative block, data not shown).

A remarkable observation of this study is that the oligomer stability was enhanced in a cation specific manner; in the presence of K^+, even heating to 95 °C could not dissociate the oligomer. From all tested cations, those with an atomic radius larger than that of K^+ (Rb^+ and Cs^+) are able to stabilize the tetramer while the smaller ones (Na^+ and Li^+) do not. This protection effect appears to be related to the permeability of the cation in question. Na^+ and Li^+, which do not pass through the channel and apparently do not enter the pore, have no stabilizing activity. On the other hand, the permeant cation Rb^+ also stabilizes the oligomer, although the stabilizing effect of Rb^+ seems to be somewhat weaker than that of K^+. Cs^+ does not permeate the channel in the bilayer, but it is able to block the conductance in a voltage-dependent manner (Figure 4). This implies that Cs^+ can enter the channel pore from at least one side; this limited accessibility of the pore to Cs^+ is consistent with the observation that also Cs^+ can partially stabilize the oligomer conformation. These cation specific modulations on the channel's oligomeric stability might be important for the interpretation of the effects of these cations on channel function. It is tempting to speculate that these interactions with the channel protein are the molecular basis for phenomena such as transmembrane block and the unusual gating in the presence of Rb^+ (see below).

These findings agree well with previous studies of KcsA (*18*). Also in this channel, the stability of the tetramer was found to be determined by the number and species of cations bound within the pore. Apparently ions which are able to enter the selectivity filter of the channel have dual roles. They are transported, and at the same time, they stabilize the delicate quaternary structure of the channel protein. This dual role occurs as a general feature of K^+ channels. Previously, it was found for native channels that a depletion of K^+ on either side of the channel results in a conformational change of the channel pore; the pore essentially collapses reversibly or even irreversibly (*22*). Similar observations were obtained from crystals of the KcsA channel, prepared in the absence of K^+. The structure determined from these crystals showed that the channel pore had become distorted (*23*). Similarly, it was found that K^+ ions were required during solubilization of voltage-dependent K^+ channels; otherwise, toxin binding (a sensitive measure of oligomeric structure) could not be assessed (*24*). Like the results seen in this study, this effect was mimicked by permeant Rb^+ but not impermeant (Li^+ and Na^+) species, while Cs^+ had an intermediate ability to retain toxin binding (*25*). Together with these data, this fosters the hypothesis that the selectivity filter contributes strongly to the oligomer stability of the channel.

Functional Properties. The viral channel has in the past been expressed in different heterologous systems, where it generated a K^+ selective conductance (*2*, *4*). However, so far, the functional analysis of the channel was all based on recordings of macroscopic currents, assuming that these were generated by the activity of ion channels. These data now show that the purified protein in planar lipid bilayers indeed exhibits the features characteristic of a K^+ selective ion channel; this confirms a canonical channel nature of this miniature membrane protein. As with other K^+ channels, the Kcv-mediated conductance switches in a stochastic manner between a closed state and discrete open channel amplitudes. Analysis of current traces containing single or multiple active copies of the Kcv protein revealed a main conductance state with less frequent subconductance levels (Figure 3C,D,F).

Table 1: Cations Block Kcv Conductance in a Different Manner Depending on Whether They Are Present on the Cis or Trans Side of the Membrane[a]

	cis				trans			
cation	type of block	affinity	voltage-dependent	TMB	type of block	affinity	voltage-dependent	TMB
Cs^+	fast	high	yes	yes	fast	low	no	yes
Na^+	–	–	–	no	fast	low	yes	yes
Ba^{2+}	slow	high	no	not detected	slow	high	no	not detected
	fast	high	yes		–	–	–	

[a] The orientation of the channel is in reference to that shown in Figure 3A. TMB stands for transmembrane block.

Worth noting is the fact that the full and sublevel conductance states are within the resolved time domain exclusively achieved from the closed state. This may be important for the future investigation of the molecular mechanism of the gate(s).

These single-channel recordings show that the open channel $I-V$ relation of Kcv has an articulate rectifying $I-V$ characteristic. In the prevailing membrane orientation (e.g., Figure 3C), the channel current increases linearly with positive voltage. In the negative voltage range, the conductance exhibits an unusual negative slope conductance. The linear section of the open channel $I-V$ relation provides information about the saturation of the Kcv conductance as a function of substrate. The extrapolated maximal conductance (360 pS) and $c_{1/2}^{\Lambda_{max}}$ value (125 mM) show that the channel has a large unitary conductance; it is in the range of the limiting conduction observed for KcsA (*26*, *27*). Only the conductance of Kcv is saturated at slightly lower KCl concentrations and displays a $c_{1/2}^{\Lambda_{max}}$ value lower than that of KcsA.

At negative voltages, the open channel amplitude of Kcv decreases, resulting at extreme negative voltages even in a negative slope conductance (Figure 3C,E). The molecular mechanisms underlying this decrease in open channel conductance remain unsolved. With the temporal resolution of the recording, it is not possible to determine whether, for example, fast gating (*28*) or conformational changes in the channel protein (*29*) are responsible for this negative slope conductance. It is possible that voltage-induced forces within the molecule lead to a distortion and consequent reduction of the open conformation (*30*).

Rectification of the open channel conductance in Kcv is different from that reported for KcsA; rectification of this channel is at negative voltages mainly due to a preferential occupancy of a smaller subconductance states, while at positive voltages, the channel preferentially switches to the larger main conductance states (*26*). In contrast to this, Kcv rectification can be clearly attributed to smaller open channel amplitudes at a V_h of <0 mV for both the main and subconductance states.

The observation that Kcv reveals typical channel gating is of particular interest in the context of the structural simplicity of the channel protein compared to other K^+ channels. Due to the very short second transmembrane domain of Kcv (*3*), the channel presumably lacks the structural prerequisite to form the pronounced crossing of the inner transmembrane domain bundles ("tepee conformation"), found in the KcsA channel (*16*). Conformational transitions in the tepee region of KcsA have been associated with the gate of this channels (*31*). The data presented here show that Kcv undergoes in spite of its structural simplicity intrinsic gating and, in the absence of the bundle crossing, show that other structures such as the selectivity filter may function as a gate (*32*, *33*).

Our data also argue for an intimate relationship between ion permeation and gating. Na^+ and Cs^+ are both unable to permeate the channel, but they are able to exert a transmembrane-like inhibition of K^+ current. This transmembrane inhibition is competitively reversed by the presence of the permeable K^+ ion. The molecular mechanisms of the transmembrane block are not readily resolved by our experimental data, but on the basis of the background of these findings, one explanation could be a competition of Cs^+ or Na^+ with K^+ for binding sites in the exit from the channel pore. The data are consistent with a model in which the channel has a high- and a low-affinity binding site for Cs^+ on the cis and trans sites, respectively. Low-affinity binding of Na^+ is only relevant on the trans site. The occupancy of the low-affinity binding sites by Na^+ or Cs^+ explains the strong reduction of the K^+ inward current in experiments with bi-ionic conditions. As soon as K^+ is present, it forces Cs^+ or Na^+ out of the respective sites and suppresses any block. Interestingly, a higher membrane voltage, which promotes the flow of K^+ ions through the channel, leads to a partial relieving of the transmembrane channel block by Cs^+ (see Figure 4A). Altogether, these data argue for one or several sites of cation specific interaction within the conductive pathway of the protein (see Table 1). Similar conclusions can be drawn from the behavior of the channel in Rb^+. These data and previous experiments reveal that Kcv is highly permeable for Rb^+ (*3*). However, transport of Rb^+ through the channel appears to lead to a change in the channel properties. In heterologous systems, the activity of the channel decreases at negative voltages in a voltage- and time-dependent manner when Rb^+ passes through the channel (*3*). In this study, we find at the single-channel level that the channel loses its clear open−closed transitions and becomes hyperconductive. Again, the data argue for an involvement of structures in the conducting pathway on this altered channel behavior. Under bi-ionic conditions, the Rb^+ effect is only apparent when Rb^+ passes through the channel. This effect can be readily reversed by a K^+ current in the opposite direction, i.e., a current, which depletes Rb^+ from the conducting pathway. The pore of potassium channels is asymmetric with respect to its global structure (*16*) and K^+ and Rb^+ binding sites (*34*). The finding that Rb^+ affects Kcv function in a similar fashion from both sides of the membrane furthermore suggests that the effect of this cation cannot be assigned to any of the asymmetrical features of the channel; therefore, the selectivity filter is a good candidate as a site

of action. Notably, the effects on the channel properties by various ions correlate with their effect on oligomer stability. Thus, only K^+ is able to fully protect the channel quaternary structure from dissociation (Figure 2). Rb^+ and Cs^+ are only weakly protective and Na^+ and Li^+ not at all protective. Hence, cations other than K^+ cause some kind of destabilization of the perfect geometry of the selectivity filter of the native channel protein. These small distortions might be sufficient to render the channel inactive with Na^+ and Cs^+ or hyperactive with Rb^+.

Single-channel bilayer recordings have a great potential to detail and complement many of the observations obtained from recordings of macroscopic Kcv currents in cellular systems. A prerequisite for this refined comparison is to define the orientation of the channel in the bilayer with respect to that in cells. These data imply that the open channel $I-V$ relation of Kcv is an inward rectifier. The argument for this assignment is the observation that Cs^+ causes a voltage-dependent block on Kcv currents only when it is added to the cis compartment but not on the trans side. Previous experiments (*2*, *3*) showed that an extracellular Cs^+ concentration as high as 10 mM had no appreciable impact on the Kcv conductance in *Xenopus* oocytes. This allows us to tentatively suggest that the Cs^+ insensitive trans side in the prevailing bilayer orientation corresponds to the external side of the channel in the cellular context.

The analysis of macroscopic currents in oocytes or HEK293 cells has shown that Kcv conductance has a defined selectivity for alkali cations with the following selectivity series: $Rb \geq K \gg Cs \gg Na$ (*3*). These data now reveal that the channel is even more selective in the bilayer system. Unlike the case in the cellular systems, the reconstituted channel has no appreciable conductance for Na^+ and Cs^+. The reason for the discrepancy between the systems could be a technical one in that the channel data in the bilayer are not contaminated with background currents. However, a more likely explanation for the discrepancy in selectivity is related to the relative hydrophobic length of the channel protein with respect to the bilayer thickness. Recent experiments showed that an extension of the hydrophobic length of the outer transmembrane domain of Kcv resulted in an increase in channel selectivity (*35*). It is reasonable to assume that the L-α-phosphatidylcholine membrane used for making lipid bilayers is thinner than that of cellular membranes, which are usually thick because of their cholesterol content. The difference in selectivity of Kcv could be caused by small conformational changes, which are required for the protein to avoid a hydrophobic mismatch in different lipid environments (*36*). Similar dependencies between bilayer thickness and channel function, including selectivity, were reported for other channel proteins (*37*, *38*).

CONCLUSION

The miniature viral K^+ channel Kcv can be expressed and purified from *P. pastoris*. The protein has a high stability as a tetramer, and this stability is maintained by those alkali cations, which can at least partially enter the pore. Reconstitution of the channel protein in planar lipid bilayers shows that the protein forms a highly cation selective Ba^{2+} sensitive channel with endogenous rectifying properties. The initial analysis reveals that the channel has some interesting functional features, including a transmembrane inhibition by Na^+ and Cs^+ ions and a modulation of the typical channel fluctuation characteristics when Rb^+ is entering the pore.

NOTE ADDED AFTER ASAP PUBLICATION

This paper posted ASAP on January 6, 2007 with typographical errors. The corrected version was published on January 23, 2007.

REFERENCES

1. Van Etten, J. L. (2003) Unusual life style of giant chlorella viruses, *Annu. Rev. Genet. 37*, 153−195.
2. Plugge, B., Gazzarrini, S., Nelson, M., Cerana, R., Van Etten, J. L., Derst, C., DiFrancesco, D., Moroni, A., and Thiel, G. (2000) A potassium channel protein encoded by chlorella virus PBCV-1, *Science 287*, 1641−1644.
3. Gazzarrini, S., Kang, M., Van Etten, J. L., DiFrancesco, D., Thiel, G., and Moroni, A. (2004) Long-distance interactions within the K^+ channel pore highlightened by molecular diversity of viral proteins, *J. Biol. Chem. 279*, 28443−28449.
4. Moroni, A., Viscomi, C., Sangiorgio, V., Pagliuca, C., Meckel, T., Horvath, F., Gazzarrini, S., Valbuzzi, P., Van Etten, J. L., DiFrancesco, D., and Thiel, G. (2002) The short N-terminus is required for functional expression of the virus-encoded miniature K^+ channel Kcv, *FEBS Lett. 530*, 65−69.
5. Gazzarrini, S., Van Etten, J. L., DiFrancesco, D., Thiel, G., and Moroni, A. (2002) Voltage-dependence of virus encoded miniature K^+-channel Kcv, *J. Membr. Biol. 187*, 15−25.
6. Libertini, G., and Di Donato, A. (1992) Computer-aided gene design, *Protein Eng. 5*, 821−825.
7. Schmidt, T. G., Koepke, J., Frank, R., and Skerra, A. (1996) Molecular interaction between the Strep-tag affinity peptide and its cognate target, streptavidin, *J. Mol. Biol. 255*, 753−766.
8. Stratton, J., Chiruvolu, V., and Meagher, M. (1998) High cell-density fermentation, *Methods Mol. Biol. 103*, 107−120.
9. Curless, C., Baclaski, J., and Sachdev, R. (1996) Phosphate glass as a phosphate source in high cell density *Escherichia coli* fermentations, *Biotechnol. Prog. 12*, 22−25.
10. Mueller, P., Chien, T. F., and Rudy, B. (1983) Formation and properties of cell-size lipid bilayer vesicles, *Biophys. J. 44*, 375−381.
11. Woodbury, D. J., and Hall, J. E. (1988) Role of channels in the fusion of vesicles with a planar bilayer, *Biophys. J. 54*, 1053−1063.
12. Hille, B. (2001) *Ion Channels of Excitable Membranes*, 3rd ed., pp 507, Sinauer, Sunderland, MA.
13. Cregg, J. M., Barringer, K. J., Hessler, A. Y., and Madden, K. R. (1985) *Pichia pastoris* as a host system for transformations, *Mol. Cell. Biol. 5*, 3376−3385.
14. Cregg, J. M., and Madden, K. R. (1989) Use of site-specific recombination to regenerate selectable markers, *Mol. Gen. Genet. 219*, 320−323.
15. Clare, J. J., Romanos, M. A., Rayment, F. B., Rowedder, J. E., Smith, M. A., Payne, M. M., Sreekrishna, K., and Henwood, C. A. (1991) Production of mouse epidermal growth factor in yeast: High-level secretion using *Pichia pastoris* strains containing multiple gene copies, *Gene 105*, 205−212.
16. Doyle, D. A., Cabral, J. M., Pfuetzner, R. A., Kuo, A. L., Gulbis, J. M., Cohen, S. L., Chait, B. T., and MacKinnon, R. (1998) The structure of the potassium channel: Molecular basis of K^+ conduction and selectivity, *Science 280*, 69−77.
17. Suzuki, H., and Terada, T. (1988) Removal of dodecyl sulfate from protein solution, *Anal. Biochem. 172*, 259−263.
18. Krishnan, M. N., Bingham, J. P., Lee, S. H., Trombley, P., and Moczydlowski, E. (2005) Functional role and affinity of inorganic cations in stabilizing the tetrameric structure of the KcsA K^+ channel, *J. Gen. Physiol. 126*, 271−283.
19. Parcej, D. N., and Eckhardt-Strelau, L. (2003) Structural characterisation of neuronal voltage-sensitive K^+ channels heterologously expressed in *Pichia pastoris*, *J. Mol. Biol. 333*, 103−116.
20. Cortes, D. M., and Perozo, E. (1997) Structural dynamics of the *Streptomyces lividans* K^+ channel (SKC1): Oligomeric stoichiometry and stability, *Biochemistry 36*, 10343−10352.

21. Heginbotham, L., Odessey, E., and Miller, C. (1997) Tetrameric stoichiometry of a prokaryotic K^+ channel, *Biochemistry 36*, 10335−10342.
22. Almers, W., and Armstrong, C. M. (1980) Survival of K^+ permeability and gating currents in squid axons perfused with K^+ free media, *J. Gen. Physiol. 75*, 61−78.
23. Zhou, Y., Morais-Cabral, J. H., Kaufman, A., and MacKinnon, R. (2001) Chemistry of ion coordination and hydration revealed by a K^+ channel-Fab complex at 2.0 Å resolution, *Nature 414*, 43−48.
24. Rehm, H., and Betz, H. (1984) Solubilization and characterization of the β-bungarotoxin-binding protein of chick brain membranes, *J. Biol. Chem. 259*, 6865−6869.
25. Parcej, D. N., and Dolly, J. O. (1989) Dendrotoxin acceptor from bovine synaptic plasma membranes. Binding properties, purification and subunit composition of a putative constituent of certain voltage-activated K^+ channels, *Biochem. J. 257*, 899−903.
26. Meuser, D., Splitt, H., Wagner, R., and Schrempf, H. (1999) Exploring the open pore of the potassium channel from S*treptomyces lividans*, *FEBS Lett. 462*, 447−452.
27. LeMasurier, M., Heginbotham, L., and Miller, C. (2001) KcsA: It's a potassium channel, *J. Gen. Physiol. 118*, 303−314.
28. Schröder, I., Harlfinger, P., Huth, T., and Hansen, U. P. (2005) A subsequent fit of time series and amplitude histogram of patch-clamp records reveals rate constants up to 1 per microsecond, *J. Membr. Biol. 203*, 83−99.
29. Berneche, S., and Roux, B. (2005) A gate in the selectivity filter of potassium channels, *Structure 13*, 591−600.
30. Krasilnikov, O. V., Merzlyak, P. G., Yuldasheva, L. N., and Capistrano, M. F (2005) Protein electrostriction: A possibility of elastic deformation of the α-hemolysin channel by the applied field, *Eur. Biophys. J. 34*, 997−1006.
31. Cortes, D. M., Cuello, L. G., and Perozo, E. (2001) Molecular architecture of full-length KcsA: Role of cytoplasmic domains in ion permeation and activation gating, *J. Gen. Physiol. 117*, 165−180.
32. Cordero-Morales, J. F., Cuello, L. G., Zhao, Y., Jogini, V., Cortes, D. M., Roux, B., and Perozo, E. (2006) Molecular determinants of gating at the potassium-channel selectivity filter, *Nat. Struct. Mol. Biol. 13*, 311−318.
33. Cordero-Morales, J. F., Cuello, L. G., and Perozo, E. (2006) Voltage-dependent gating at the KcsA selectivity filter, *Nat. Struct. Mol. Biol. 13*, 319−322.
34. Nimigean, C. M., and Miller, C. (2002) Na^+ block and permeation in a K^+ channel of known structure, *J. Gen. Physiol. 120*, 323−335.
35. Hertel, B., Tayefeh, S., Mehmel, M., Kast, S. M., Van Etten, J., Moroni, A., and Thiel, G. (2006) Elongation of outer transmembrane domain alters function of miniature K^+ channel Kcv, *J. Membr. Biol. 210*, 21−29.
36. de Planque, M. R., Boots, J. W., Rijkers, D. T., Liskamp, R. M., Greathouse, D. V., and Killian, J. A. (2002) The effects of hydrophobic mismatch between phosphatidylcholine bilayers and transmembrane α-helical peptides depend on the nature of interfacially exposed aromatic and charged residues, *Biochemistry 41*, 8396−8404.
37. Tillman, T. S., and Cascio, M. (2003) Effects of membrane lipids on ion channel structure and function, *Cell Biochem. Biophys. 38*, 161−190.
38. Garavaglia, M., Dopinto, S., Ritter, M., Furst, J., Saino, S., Guizzardi, F., Jakab, M., Bazzini, C., Vezzoli, V., Dossena, S., Rodighiero, S., Sironi, C., Botta, G., Meyer, G., Henderson, R. M., and Paulmichl, M. (2004) Membrane thickness changes ion-selectivity of channel-proteins, *Cell Physiol. Biochem. 14*, 231−240.

BI061530W